Enhanced degradation of perfluorooctanoic acid by heat-activated persulfate in the presence of zeolites

Lin Qian[a], Frank-Dieter Kopinke[a], Tom Scherzer[b], Jan Griebel[b] and Anett Georgi[a]*

[a] Helmholtz Centre for Environmental Research – UFZ, Department of Environmental Engineering, Permoserstr. 15, D-04318, Leipzig, Germany

[b] Leibniz Institute of Surface Engineering (IOM), Material Characterization and Analytics, Permoserstr. 15, D-04318, Leipzig, Germany

Corresponding author e-mail: anett.georgi@ufz.de

Abstract

The treatment of contaminations with perfluorooctanoic acid (PFOA) is a huge challenge due to its environmental persistence and global distribution. A combination of adsorption and degradation processes is considered as a promising approach for removing PFOA traces from water. In the present study, we developed a novel treatment strategy for PFOA using heat-activated persulfate in the presence of BEA35 - a BEA-structure type zeolite. Our experimental results show for the first time that BEA35 not only removes PFOA by adsorption, but also accelerates its degradation by means of heat-activated persulfate until complete mineralization. The presence of zeolite (50 g L^{-1}) increases PFOA degradation up to 99.8% compared with 58% in homogeneous solution under the same reaction conditions ($C_{0,\text{persulfate}}$ = 100 mM, 90 min, 70 °C). The influence of reaction conditions such as pH value, zeolite dosage and type were investigated, and possible reaction mechanisms were considered. The applicability of the zeolite-based treatment system was verified with real groundwater samples. A first cost estimation was provided for the application case of a zeolite fixed-bed adsorber with intermittent regeneration by heat-activated persulfate. The presented approach has the potential to overcome several shortcomings of the existing PFOA degradation technologies, such as high energy demands, vulnerability in complex water matrices, and inefficiency at trace concentration levels. Our findings provide an effective and efficient strategy for treatment of water containing traces of PFOA, which can also inspire the development of remediation technologies for water contaminated by other micropollutants.

Keywords: Perfluorooctanoic acid; Heat-activated persulfate; Trap & treat principle; Zeolite adsorption; Cost estimation.

1. Introduction

Per- and polyfluoroalkyl substances (PFAS) are emerging persistent organic pollutants (POPs), which cause environmental problems as they are reported not to be eliminated in wastewater treatment plants [1]. Recent studies show that the exposure of PFAS at certain levels may cause adverse effects on human health [2, 3]. Although the production and application of PFAS is currently restricted, the possible risk of human exposure due to their accumulation in the environment will continue to exist over a long period of time [4]. Even worse, the treatment of PFAS in the environment is a huge challenge. Firstly, PFAS concentration in natural water bodies are rather low, i.e. usually at or even below the ng L^{-1} level [5]. Chemical treatment of such low concentrations is usually inefficient, so a pre-enrichment process is necessary. Secondly, PFAS are rather resistant to most conventional oxidation, reduction and biological degradation processes, mainly due to the very strong carbon-fluorine bonds ($D_{C\text{-}F} \approx 485$ kJ mol^{-1}) [6]. Among various PFAS, perfluorooctanoic acid (PFOA) is one representative perfluorinated carboxylic acid (PFCA), which has drawn much attention recently due to its frequent detection in the environment. PFOA and its most important pre-cursors have been banned by the Stockholm convention since 2019; however, exceptions were made for various industries such as in semiconductor manufacturing or polytetrafluoroethylene (PTFE) production for various purposes. Thus, and due to previous accumulations, efficient and cost-effective PFOA degradation techniques are urgently needed for treating e.g. wastewaters and contaminated natural waters.

Several current technologies can remove PFOA from water, e.g. activated carbon adsorption, reverse osmosis and ion exchange [7]. In these cases, PFOA-enriched solutions or solids are produced and need to be further treated. Taking the activated carbon as an example, the common way to treat exhausted activated carbon is incineration or, if possible, high-temperature

regeneration in specialized treatment plants with suitable off-gas treatment.

Beside the PFOA *removal* technologies, several PFOA *degradation* technologies have been studied recently, e.g. oxidation by activated persulfate or peroxymonosulfate, electrochemical, sonochemical, photochemical, and photocatalytic treatment [8]. These technologies can degrade or even fully mineralize PFOA within acceptable time; however, the relatively high energy demands and operation costs have been limiting their practical application.

In PFOA degradation by activated persulfate ($S_2O_8^{2-}$) or peroxymonosulfate (SO_5^{2-}), sulfate radicals are considered as the main reactive species. Hori et al. [9] first reported an efficient degradation of PFOA and shorter-chain perfluorocarboxylic acids (PFCAs) using persulfate as a photochemically activated oxidant (eq.1).

$$S_2O_8^{2-} \xrightarrow{h\upsilon} 2SO_4^{-}\cdot \qquad (1)$$

The produced sulfate radicals attack PFOA by a one-electron transfer step. Similarly, persulfate can also be thermally activated at elevated temperatures ($T \geq 50$ °C) (eq.2) [10]. In addition, it can be chemically activated in homogeneous or in heterogeneous media upon use of activators such as dissolved transition metals [11] and metallic materials [12-15].

$$S_2O_8^{2-} \xrightarrow{\Delta} 2SO_4^{-}\cdot \qquad (2)$$

The persulfate-based processes were also widely used in environmental remediation for treating other kinds of contaminants, e.g. pesticides, pharmaceuticals and personal care products [16]. In several cases, high reaction stoichiometric efficiency (%RSE) was observed [17-19], which is the molar ratio of target compound degraded per oxidant consumed. However, in case of PFCAs the efficiency of persulfate-based processes is strongly limited by the low reaction rate constant of the primary single-electron transfer step, which is about $k_{SO_4^{-}\cdot} = (1.7\text{-}4.4) \times 10^4$ $M^{-1}s^{-1}$ [20]. This

implies low radical utilization rates in the presence of coexisting radical consumers such as certain inorganic anions (e.g. chloride and carbonate) and organic compounds [20]. Thus, a preceding selective enrichment of PFOA by adsorption to an inert adsorbent material is a promising option for improved efficiency of persulfate-based processes.

Zeolites are microporous minerals with certain framework structures, which are commonly applied as catalysts and adsorbents. PFAS adsorption by zeolites has been investigated by various researchers. Van den Bergh et al. [21] recently investigated the performance of an all-silica BEA type zeolite for selective removal of PFOA and perfluorooctanesulfonic acid (PFOS). They claimed the adsorption of PFOA and PFOS to be driven by favorable steric factors and negative adsorption enthalpy. Qian et al. established an adsorption-degradation approach for removal of PFOA and PFOS from a real groundwater sample using Fe-doped zeolites (Fe-BEA35) [22, 23]. In this process, Fe-BEA35 not only shows a high adsorption affinity toward PFOA and PFOS, but also acts as a photocatalyst, which can be regenerated by photochemical degradation of PFOA and PFOS under UV irradiation. Since sulfate radicals are known to degrade PFOA, it is of great interest whether a combined process, i.e. heat-activated persulfate for degradation of PFOA adsorbed to zeolites, can be used to effectively treat PFOA contaminations in water.

In the current study, we chose one synthetic, commercial BEA framework type zeolite, BEA35, which presents high PFOA adsorption affinity, for detailed studies, but also included further BEA and FAU zeolites for comparison. For the first time, PFOA adsorption and zeolite regeneration with heat-activated persulfate were combined. Our experimental results show that BEA35 accelerates PFOA degradation in the adsorbed state. Several aspects were investigated: I) effects of reaction pH and zeolite dosage on the removal/degradation performances; II) %RSE evaluation under different persulfate dosages and activation temperatures; III) possible mechanisms

explaining the promoted PFOA degradation process; and IV) stability of the system and tests with real groundwater. These findings contribute to a promising strategy for treatment of water containing trace PFOA by combined adsorption and oxidation.

2. Materials and methods

2.1. Chemicals and materials

All chemicals were in reagent grade or higher and used as received, where not otherwise stated. Deionized (DI) water was used for solution and suspension preparation in this work. Methanol was acquired from (Th. Geyer, Chemsolute). Sodium persulfate (99% purity, $Na_2S_2O_8$), perfluorobutyric acid (98% purity, PFBA, C_3F_7COOH) and perfluorooctanoic acid (96% purity, PFOA, $C_7F_{15}COOH$) were acquired from Sigma Aldrich. Perfluoropropionic acid (97% purity, PFPrA, C_2F_5COOH), perfluoropentanoic acid (97% purity, PFPeA, C_4F_9COOH) and perfluorohexanoic acid (98% purity, PFHeA, $C_5F_{11}COOH$) were acquired from J&K Scientific. Trifluoroacetic acid (99% purity, TFA, CF_3COOH) was acquired from Fluka. Perfluoroheptanoic acid (97% purity, PFHpA, $C_6F_{13}COOH$) was acquired from Alfa Aesar. In addition, the technical PFOA that contains a higher proportion of branched PFOA isomers was acquired from Haihang Industry (China). The PFOA isomer standards were acquired from Wellington Laboratories (Canada).

The zeolites BEA24 and BEA35 were acquired from Clariant Produkte GmbH (Germany). The zeolites BEA28, BEA40, BEA100 and FAU15 were acquired from Tosoh Corporation (Japan). The BEA framework contains two types of channels with 12 Si or Al atoms, i.e., with openings of a diameter (Ø) of 6.6 – 6.7 Å for the straight and Ø 5.6 – 5.7 Å for the zig-zag form channels, respectively, whereas the pore volume of the FAU framework consists mainly of large cages with

Ø around 11 Å. The numbers in the zeolite type names represent SiO_2/Al_2O_3 molar ratios. The XRD pattern of BEA35 was measured, which was in good agreement with the BEA framework type as shown in Figure S1. More detailed information about these zeolites including morphology, particle size and BET surface areas are presented in the SI.

2.2. PFOA degradation experiments

Degradation of PFOA by heat-activated persulfate in the presence and in the absence of zeolites was conducted in sealed 40 mL glass flasks. For most experiments, an aqueous PFOA solution (30 mL, 240 μM) was mixed with 1.5 g zeolite in the flask followed by 2 h shaking to achieve adsorption equilibrium. About 99.9% of PFOA was in the adsorbed state. Before start of reaction, the flasks containing PFOA solutions or zeolite suspensions were preheated in a water bath, where a reaction temperature of 70 °C was maintained. When the temperature of the PFOA solutions or zeolite suspensions was stabilized, the reaction was initiated by introducing certain amounts of sodium persulfate.

The real groundwater samples had very low PFOA concentrations, ranging from 35 to 82 ng L^{-1}. The PFOA was enriched from groundwater samples by the zeolite thanks to its high adsorption affinity towards PFOA. Figure S2 shows in a scheme how the PFOA-containing groundwater samples were treated before the reaction. 1 L of groundwater was filtered through a 0.45 μm paper filter for removal of large particles. The chemical composition of groundwater samples after filtration is shown in Table S1. The filtered groundwater sample was then mixed with 0.5 g BEA35 zeolite and shaken for 1 day. The majority of PFOA was adsorbed by the zeolite after 1 day. For determination of very low PFOA concentrations, aqueous samples were concentrated by evaporation. The concentration of dissolved PFOA after adsorption was below the detection limit of the LC-MS measurement (50 ng L^{-1}) even after evaporative concentration by two orders of

magnitude. The suspension was kept standing for 2 days, after which the supernatant was discarded completely. The PFOA-loaded zeolite particles were then washed once by 50 mL DI water, and the supernatant was removed by centrifugation at 2500 rpm for 5 min. After that, the washed PFOA-loaded zeolite particles were re-suspended with 10 mL DI water and collected for the further treatment. Almost no inorganic ions (e.g. sulfate, chloride and carbonate) were detected in the resulting zeolite suspension. After this, an enrichment factor of 10^2 for PFOA was achieved (from 1 L to 10 mL) and the final zeolite concentration was 50 g L^{-1}.

For zeolite reusability tests, the supernatant was removed after each reaction period (90 min) by centrifugation at 2500 rpm for 5 min. The remaining zeolite particles were re-suspended in the fresh aqueous PFOA solution. The suspension was prepared for the next reaction run after shaking for 2 h for adsorption equilibration.

2.3. Extraction of PFOA and intermediates from zeolites

After sampling of zeolite suspensions, methanol was added to the sample both to scavenge radicals and to extract PFOA and intermediates from zeolites as previously described [24]. 2 mL of methanol was added to a 100 μL zeolite suspension aliquot in a 4 mL tube. After shaking overnight, the mixture was centrifuged at 2500 rpm for 5 min. The supernatant was taken and analyzed by means of LC-MS in order to determine the total PFOA and intermediate concentrations (adsorbed and freely dissolved fractions). This extraction procedure can achieve almost a complete recovery ((94 ± 2) %) of PFOA from a sample after 2-h adsorption. Most of the fluoride produced during the reaction was released into the aqueous phase. The remaining fluoride in the zeolites was extracted by adjusting suspension pH to 12. After the centrifugation, the supernatant was subjected to analysis by means of ion chromatography (IC, DX500, Thermo Fisher).

2.4. Chemical analysis

Quantitative analysis of PFOA and its degradation intermediates, i.e. PFHpA, PFHeA, PFPeA, and PFBA, was performed with LC/MS (LCMS-2020, SHIMADZU Corp.). The detailed procedure for LC/MS was described in a previous work [23]. The correlation coefficients (R^2) of the calibration curves for PFOA, PFHpA, PFHeA, PFPeA and PFBA were ≥0.99 for concentration ranges of 1 μg L^{-1} - 1 mg L^{-1}. The limit of detection for PFOA was around 50 ng L^{-1}. The standard deviations of single values were obtained from triplicate assay results. For the technical PFOA containing higher proportions of branched PFOA isomers, an isocratic LC/MS method with 45% solvent A (20 mM ammonium acetate in 90 vol-% DI water and 10 vol-% methanol) and 55% solvent B (20 mM ammonium acetate in 90 vol-% methanol and 10 vol-% DI water) was performed in order to separate the branched PFOA isomers. The running time for each measurement was 38 min. Quantitative analysis of PFPrA, TFA and fluoride was performed with IC. The analysis of octanol was performed on a GC/MS device (GCMS-QP2020, SHIMADZU Corp.). The determination of persulfate concentration was conducted with spectrophotometry by measuring the absorbance of I_3^- at 352 nm [25]. The 2θ/ω XRD pattern was measured with a diffractometer (ULTIMA IV, Rigaku) in out-of-plane geometry with parallel beam optics. Cu Kα radiation with λ= 0.15406 nm was used for the measurements. The diffractometer was equipped with a scintillation detector.

3. Results and discussion

3.1. Degradation of PFOA by heat-activated persulfate in the presence and in the absence of BEA35 zeolite.

Previous studies reported that sulfate radicals are able to react with PFCAs leading to stepwise

chain-shortening [20, 24, 26]. Based on these studies, the generally accepted mechanism is that sulfate radicals attack the carboxylic head group of PFCAs by a one-electron transfer to generate carboxylic radicals (eq. 3) followed by decarboxylation, yielding perfluorinated alkyl radicals ($\bullet C_nF_{2n+1}$) and CO_2 (eq. 4). The $\bullet C_7F_{15}$ radicals react preferentially with dissolved O_2 to produce the peroxyl radical ($C_7F_{15}OO\bullet$) (eq.5). Through several radical reactions and hydrolysis processes, a PFCA with one CF_2 unit less will be produced (eqs. 6 - 10). The produced shorter-chain PFCAs continue to be attacked by sulfate radicals and finally a complete mineralization of PFCAs can be achieved.

$$C_7F_{15}COO^- + SO_4^-\bullet \longrightarrow C_7F_{15}COO\bullet + SO_4^{2-} \quad (3)$$

$$C_7F_{15}COO\bullet \longrightarrow \bullet C_7F_{15} + CO_2 \quad (4)$$

$$\bullet C_7F_{15} + O_2 \longrightarrow C_7F_{15}OO\bullet \quad (5)$$

$$2C_7F_{15}OO\bullet \longrightarrow C_7F_{15}OO\text{-}OOC_7F_{15} \quad (6)$$

$$C_7F_{15}OO\text{-}OOC_7F_{15} \longrightarrow 2C_7F_{15}O\bullet + O_2 \quad (7)$$

$$C_7F_{15}O\bullet + HSO_4^- \longrightarrow C_7F_{15}OH + SO_4^-\bullet \quad (8)$$

$$C_7F_{15}OH \longrightarrow C_7F_{13}OF + HF \quad (9)$$

$$C_7F_{13}OF + H_2O \longrightarrow C_6F_{13}COOH + HF \quad (10)$$

In this section, we compare PFOA degradation by heat-activated persulfate in the homogeneous and heterogeneous systems, whereby in the latter zeolite functions as an adsorbent of PFOA. A typical homogeneous system contained 100 mM persulfate and $C_{0,PFOA}$ = 240 μM. A heterogeneous system contained in addition 50 g L^{-1} BEA35 zeolite, whereby PFOA exists predominantly in the adsorbed state (99.9%) after 2 h equilibration. The initial pH values of both systems were adjusted to pH_0 = 3.0. The total concentration of PFOA in zeolite suspension (including freely dissolved and adsorbed fractions) was obtained via a solvent extraction step (as

described in Section 2.3). As shown in Figure 1(a), 99.8% degradation and 71% defluorination of the initial 240 μM PFOA was achieved in the presence of zeolite within 90 min compared to 58% degradation in the absence of zeolites under identical conditions. Thus, PFOA degradation by heat-activated persulfate was significantly promoted in the presence of zeolite. When describing the PFOA degradation kinetics with a pseudo-first-order kinetics, the acceleration effect is a factor of about 7 (= ln(100/0.2)/ln(100/42), see below).

In general, two types of reactions in the presence of zeolite should be considered, i.e. homogeneous reaction in the solution phase and heterogeneous reaction, i.e. reaction of adsorbed PFOA inside the zeolite. The fractions of adsorbed PFOA (X_{sorb}) and freely dissolved PFOA (X_{free}) can be described as follows:

$$X_{sorb} = 1 - X_{free} \tag{11}$$

$$X_{free} = C_{PFOA,free} / C_{PFOA} \tag{12}$$

Based on eq. 3, a rate eq. 13 can be derived:

$$-\frac{dC_{PFOA}}{dt} = k_1 \cdot C_{PFOA} \cdot X_{sorb} \cdot C_{zeolite,SO_4^{\cdot-}} + k_2 \cdot C_{PFOA} \cdot X_{free} \cdot C_{bulk,SO_4^{\cdot-}} \tag{13}$$

where k_1 and k_2 are the rate constants for reaction of adsorbed and freely dissolved PFOA with sulfate radicals, respectively and $C_{zeolite,SO_4^{\cdot-}}$ and $C_{bulk,SO_4^{\cdot-}}$ are the concentrations of sulfate radicals (per total water volume) produced by thermal activation of persulfate inside the zeolite and in the bulk phase, respectively. However, the values of $C_{zeolite,SO_4^{\cdot-}}$ and $C_{bulk,SO_4^{\cdot-}}$ cannot be easily determined. The fractions of X_{sorb} and X_{free} can be experimentally obtained. For instance, under the condition of $C_{zeolite}$ = 50 g L^{-1} and $C_{0,PFOA}$ = 240 μM, X_{free} = 0.002 was much smaller than X_{sorb} = 0.998. In this case, the homogeneous reaction in the bulk phase can be ignored, and eq. 13 results in the simplified rate eq. 14:

$$-\frac{dC_{PFOA}}{dt} = k_1 \cdot C_{PFOA} \cdot C_{zeolite,SO_4^{\cdot-}} \quad (14)$$

It is worth noting that, under the described conditions, the initial period of PFOA degradation (0 – 60 min) in the presence of zeolite can be well fitted by pseudo-first-order kinetics ($R^2 = 0.998$, Figure S3), which is in accordance with the reaction kinetics described by eq. 14 considering that persulfate turnover is still very low and thus $C_{zeolite,SO_4^{\cdot-}} \approx$ constant. The apparent rate constant decreases slightly at high PFOA turnover (> 99% at t > 60 min).

To further confirm that a heterogeneous reaction dominates the PFOA degradation in the presence of zeolite, we compared the degradation of PFOA with a shorter-chain PFCA, i.e., PFBA. It has the same carboxylic group as PFOA but with a shorter carbon chain length. As a consequence, zeolites have much weaker adsorption affinity for PFBA due to weaker hydrophobic interactions, as reported in our previous work [22, 23]. Under these conditions ($C_{zeolite}$ = 50 g L^{-1} and $C_{0,PFBA}$ = 240 μM), only 23% of PFBA was adsorbed after 2 h equilibration. As shown in Figure 1(b), the degradation rates of PFOA and PFBA were almost identical in the homogeneous systems. This is not surprising because the sulfate radicals attack PFCAs at the carboxylic head group, which is the same for PFOA and PFBA [20]. The different carbon chain lengths are not decisive in the initial reaction step. However, in the presence of zeolite, the degradation of PFOA was much faster than that of PFBA, where the majority of PFOA was adsorbed onto the zeolite but PFBA was dominantly present in the aqueous phase. This is clear evidence that in the presence of zeolites, PFOA degradation takes place via a heterogeneous reaction inside the zeolite. Since the PFOA degradation was significantly increased after its adsorption to BEA35, it can be supposed that BEA35 zeolite may not only be an adsorbent of PFOA but also a catalyst for its degradation. More detailed investigation of this promotion effect is discussed in the following sections.

In order to elucidate the PFOA degradation mechanism, the concentrations of the intermediates produced during the reaction were analyzed. Six shorter-chain PFCAs were identified and quantified by means of IC (C2 and C3) and LC/MS (C4 to C7) analysis. Their concentration profiles along the reaction time are displayed in Figure 2(a). The PFCAs with longer chains, e.g. C5 to C7, reached their maximal concentrations at earlier stages (< 60 min) and then diminished gradually, while shorter-chain PFCAs were increasingly detected. This indicates that longer-chain PFCAs are degraded stepwise towards shorter-chain PFCAs. Additionally, the degradation of shorter-chain PFCAs is slower, most likely due to their lower adsorption affinities to zeolite. In fact, the degradation of shorter-chain PFCAs, e.g. C2 and C3, probably took place outside the zeolite in the water bulk phase.

The fluorine mass balance during PFOA degradation in the heat-activated persulfate/zeolite system is shown in Figure 2(b). The fluorine in the system is classified into four groups: fluoride, C2 to C4 PFCAs, C5 to C7 PFCAs and the remaining PFOA. The initial fluorine (i.e. PFOA) recovery of (94 ± 2)% was obtained by methanol extraction (see experimental part). After 3 h of reaction, a final fluorine recovery of (84 ± 3)% was obtained, which consisted mainly of fluoride and minor contributions of C2 and C3 PFCAs. In addition, the GC/MS headspace analysis did not reveal volatile fluorinated and non-fluorinated compounds produced during the process. The incomplete fluorine mass balance may be due to the formation of some undetected fluorine-containing compounds, which may be strongly bound in the zeolite and could not be extracted.

3.2. Effect of pH

We tried to fit degradation curves under both conditions (with and without zeolite) according to eq. 14 in section 3.1 in order to discuss the pH effect on reaction kinetics in this section. The initial reaction period (0 – 60 min) in the presence of zeolite can be well fitted by first-order kinetics; this

is not the case in the absence of zeolite, where an apparent zero-order kinetics is more appropriate. The thermal decomposition of persulfate causes a decrease in solution pH due to the reaction stoichiometry given by eq. 15 [27]:

$$S_2O_8^{2-} + H_2O \xrightarrow{\Delta} 2SO_4^{2-} + 2H^+ + \frac{1}{2}O_2 \quad (15)$$

In unbuffered systems applying 100 mM persulfate with initial pH_0 = 3.0, the final solution pH after 90-min reaction decreased to around 1.5 with and without zeolites (Figure S4). The decreasing pH may have an effect on the rate of PFOA degradation. Therefore, we tried to maintain the pH between 2.5 and 3.0 in both cases by manually adding NaOH solution. As seen in Figure 3(a) and (b), PFOA degradation in the presence of zeolite with buffered reaction pH showed almost identical degradation rates compared with the unbuffered conditions. However, in the absence of zeolite, PFOA degradation slowed down with buffered reaction pH. Interestingly, under buffered conditions, the PFOA degradation in the absence of zeolite can now also be fitted by a first-order kinetics (R^2 = 0.99). Hence, deviations from first-order kinetics in the unbuffered solution were due to the superimposed pH effect. This effect has also been observed by other researchers [27]. However, the pH effect was largely attenuated in the presence of zeolite.

Furthermore, we investigated PFOA degradation by heat-activated persulfate in the presence of zeolite at various initial pH values, i.e. pH_0 = 3.0, 5.0, and 7.0. As shown in Table S2, the initial adsorbed fractions of PFOA (X_{sorb}) on BEA35 zeolite are ≥ 0.998 under all tested conditions. Comparing with the rate at pH_0 = 3.0, the PFOA degradation slowed down somewhat at pH_0 = 5.0 and 7.0, resulting in 1.2 and 1.6 times higher PFOA half-life, respectively (Figure 3(c)). Overall, the pH effect is much less pronounced in the presence of the zeolite (i.e. with PFOA predominantly adsorbed) than in the homogeneous heat-activated persulfate system. Further discussion on the mechanistic basis of the pH effect is presented below.

3.3. Role of internal vs. external zeolite surface

In Section 3.1, it is mentioned that the zeolite may promote PFOA degradation by heat-activated persulfate. In fact, both linear and branched PFOA isomers are formed during the production of PFOA using electrochemical fluorination [28]. Our preliminary experiments indicate that BEA35 has a stronger adsorption affinity towards linear PFOA than towards some branched isomers due to the steric effect, i.e. size exclusion by the zeolite pore structure with channel openings of 0.56 – 0.67 nm. It is interesting to know whether the internal surface or the external surface of the zeolite particles promotes the PFOA degradation. [29]. The adsorption of linear and branched PFOA isomers would be nearly identical on the external surface, yet only linear PFOA and certain branched PFOA isomers can access the internal surface. In order to provide comparable conditions in the experiments, the branched PFOA isomers were enriched to a similar concentration range as for linear PFOA by means of selective adsorption onto zeolites (for details, see Experimental Part in SI). Some LC/MS chromatograms from degradation of PFOA mixtures with and without zeolites are shown in Figure 4. PFOA isomer standards were used for peak assignment (Figure S5). As can be seen, the degradation rates of linear PFOA and branched isomers are almost identical in the homogeneous system. This is not surprising as the PFOA degradation by sulfate radicals starts at the carboxylate group (eq. 3), which is identical in all PFOA isomers. In the presence of zeolite, the linear PFOA and certain mono-branched PFOA isomers, i.e. 5m-PFOA and 6m-PFOA, exhibit higher degradation rates than those of di-branched PFOA isomers, i.e. 5,5m-PFOA and 4,5m-PFOA. The symbol ‘m’ stands for branching by one or two CF_3 groups in the respective positions in the PFOA molecule. These findings are a clear indication that the promotion of PFOA degradation by heat-activated persulfate takes place on the internal surfaces in the pores rather than the external surfaces of the zeolite.

3.4. Variation of substrate, zeolite dosages or types and activation temperatures

In order to elucidate possible reasons for the promoting effect of zeolite on PFOA degradation, several comparison experiments were conducted. Our first hypothesis suggested that the persulfate decomposition rate might be enhanced in the presence of zeolite, which would result in promoted PFOA degradation. Thus, we monitored the concentration of persulfate during thermal activation with and without zeolites. As shown in Figure S6, the persulfate decomposition kinetics are almost identical in both cases. It seems that the presence of zeolite is irrelevant for the overall persulfate decomposition rate. However, with a concentration of 50 g L^{-1} BEA35, the zeolite pore volume amounts to less than 3% of the total volume: 97% is bulk water phase. This means that, even with a factor of 3 increase in persulfate decomposition rate constant inside the zeolite, the overall enhancement of persulfate decomposition will still be within the error range (<10%) as the observable rate constant $k_{obs,persulfate}$ would be equal to the summed products of internal/external rate constants and fractions of persulfate. Therefore, this test cannot clarify whether the persulfate decomposition rate inside the zeolite was enhanced or not. Thus, another experiment was designed in which we replaced PFOA by n-octanol. Similarly to PFOA, n-octanol can be well adsorbed on BEA35 zeolite. Unlike PFOA, n-octanol is attacked by sulfate radicals through hydrogen abstraction [30]. Nevertheless, we used here n-octanol oxidation as a probe reaction for sulfate radicals in the zeolite pores. As can be seen in Figure S7, the presence of zeolite suppressed the octanol degradation. This indicates that the accelerating effect is related to the substrate PFOA rather than the enhancement of persulfate decomposition into free sulfate radicals.

We tested various dosages of zeolites (from 0.5 to 100 g L^{-1}) with the same initially dissolved PFOA concentration, as shown in Figure 5 and Table 1. In general, the presence of zeolites promotes PFOA degradation even at the lowest zeolite dosage (0.5 g L^{-1}), where due to $X_{sorb,PFOA}$

= 0.58 the PFOA degradation reaction occurred in both compartments, i.e. inside the zeolite and in the aqueous bulk phase. A much lower PFOA degradation rate constant was observed at $C_{zeolite}$ = 0.5 g L^{-1} than in other cases with higher zeolite dosages. Note that the diffusion of persulfate between bulk phase and pore volume is relatively fast, i.e. with a characteristic diffusion time in the order of 10^{-4} s for 0.5 μm distance (= average BEA35 zeolite particle diameter). Therefore, the lower PFOA degradation rate constant cannot be explained by persulfate depletion in the zeolite pores. When we kept the initial PFOA concentration constant and increased the zeolite dosages to 5 - 100 g L^{-1}, the PFOA was predominantly adsorbed on zeolites (X_{free} < 0.015, see Table 1). Under these conditions, the PFOA degradation rate constants were significantly enhanced. The acceleration of PFOA degradation by heat-activated persulfate is more pronounced when higher zeolite dosages are applied. Additionally, when the zeolite dosage was kept constant at 50 g L^{-1} and the initial PFOA concentration was decreased from 240 to 2.4 μM, the PFOA degradation rate constants were almost identical under both sets of conditions (Figure S8), i.e. the same accelerating effect was observed from 100-fold different PFOA loadings on zeolite.

In addition to BEA35, other BEA type zeolites with various SiO_2/Al_2O_3 ratios, i.e. BEA24, BEA28, BEA40, and a zeolite of another framework type (faujasite), i.e. FAU15, were chosen in order to compare their effects on PFOA degradation by heat-activated persulfate. In general, in the presence of all types of zeolites, PFOA was predominantly adsorbed (> 99%), indicating that the heterogeneous degradation reaction should be dominant in all cases. In addition, as shown in Figure 6, all types of zeolites can promote PFOA degradation in comparison with the homogeneous system when identical conditions (including initial pH) are applied. The ranking in the PFOA degradation rate constants is BEA35 > FAU15 > BEA28 > BEA24 > BEA40, with a factor of 4 between the highest (BEA35) and lowest (BEA40) rate constant, as shown in Table S3. SEM

images of zeolite particle morphology are shown in Figure S9, while information on primary particle sizes (between 125 and 540 nm) and BET surface areas (between 510 and 660 $m^2\ g^{-1}$) is presented in Table S3. No clear correlation between any one of these parameters and the catalytic effect of the zeolites is obvious. Additionally, the contents of Brønsted acid sites (BAS) and Lewis acid sites (LAS) were determined by means of IR measurements after pyridine adsorption (detailed procedures are described in SI, Experimental Section). The IR spectra and the calculated LAS and BAS contents of the zeolites are presented in Figure S10 and Table S4, respectively. As expected, the number of BAS in BEA zeolites increases with increasing Al content (decreasing SiO_2/Al_2O_3 ratio), as each Al in the structure creates a negatively charged site which is protonated in dry H-form zeolites and attracts protons or other cations when suspended in water. A higher number of BAS in BEA zeolites also corresponds to a lower native suspension pH (Table S4). In contrast, the number of LAS seems not to correlate to the SiO_2/Al_2O_3 ratio. LAS are mainly assigned to coordinatively unsaturated (extra-framework) Al^{3+} species in zeolites, and thus could also play a role for interacting with PFOA anions. However, no significant correlation between either BAS or LAS numbers of the zeolites and their promoting effect on PFOA degradation was found.

In addition, we tested the effect of temperature on PFOA degradation by heat-activated persulfate in the presence of zeolite. As seen in Figure 7, PFOA degradation rates increased by raising the activation temperature from 50 to 90 °C. Increased temperature not only enhanced the rate of persulfate decomposition, but also facilitated the PFOA degradation, so that an overall improved PFOA degradation rate was achieved. The presence of zeolite promoted the PFOA degradation over the investigated temperature range from 50 to 90 °C. We fitted the degradation curves at various activation temperatures according to Eq. 14 in Section 3.1. using the initial reaction period for fitting. As seen in Figure 7 and Table S5, the initial observable rate constant

$k_{obs,PFOA}$ increased due to the presence of zeolite by factors of 11, 9 and 5, at activation temperatures of 50, 70 and 90 °C, respectively. In addition, reaction stoichiometric efficiency (% RSE) of the system was calculated for PFOA degradation of 80 to 90% at different activation temperatures. A higher %RSE (7.6%) at 50 °C activation temperature in the presence of zeolite was observed comparing with RSE of 3.6% and 3.4% at 70 and 90 °C, respectively (Table S5). Overall, acceleration of PFOA degradation ($k_{PFOA,zeolite}/k_{PFOA,homo}$) and persulfate utilization efficiency (% RSE) by the zeolite become most significant at the lowest temperature (50 °C). In further work, even lower temperatures (≤ 25°C) will be tested to provide relevant suggestions for *in-situ* PFCA remediation techniques.

3.5. Mechanistic consideration of accelerated PFOA degradation by heat-activated persulfate in the presence of zeolite

From the observations described above we conclude that: I) all zeolites that were able to adsorb PFOA accelerated its degradation by heat-activated persulfate, with some differences which, however, could not be assigned to specific structural parameters; II) if certain catalytic sites were to be relevant, their number does not appear to be significantly limited, as the accelerating effect was the same for 100-fold different PFOA loadings on zeolite and also did not vary significantly with increasing zeolite concentration after PFOA adsorption degree ≥ 90% was reached; III) the conditions for persulfate decomposition into free radicals inside the zeolite pores are not necessarily beneficial in general, as another substrate, i.e. n-octanol, was inhibited in its degradation when adsorbed to zeolite; and IV) the pH effect, i.e. decreasing PFOA degradation rates with increasing pH, was much less pronounced for the heterogeneous compared to the homogeneous reaction.

Sulfate radical attack by electron transfer from the carboxylic head group of PFOA is considered to be the main initial reaction step in PFOA degradation by heat-activated persulfate [10, 20, 26]. It is interesting to consider the findings and hypotheses of Bruton and Sedlak [27] in terms of the pH-effect in PFOA degradation in the homogeneous heat-activated persulfate system. In their system, consumption of sulfate radicals by OH^- became relevant only at alkaline pH. An impact of OH^- is also not expected for the homogeneous reaction under the conditions applied in this study. In addition, Bruton and Sedlak noted that persulfate decomposition rates are nearly independent of pH in the range of 8 to 2 and only slightly affected by acid catalysis below pH 2. Thus, they suggested three hypotheses for the acceleration of PFOA degradation by heat-activated persulfate with decreasing pH: I) protonation of the PFOA anion improves its reactivity towards sulfate radicals, as the reaction of two negatively charged species could be detrimental; II) protonation of sulfate radicals improves their reactivity with PFOA anions; and III) acid catalysis occurs in the reaction between PFOA and sulfate radical. The pK_a values of PFOA (-0.5 to 1 [31, 32]) and sulfate radicals (estimated below 2) are uncertain, which makes differentiation between these hypotheses difficult. Nevertheless, it is hard to accept one of these hypotheses for aqueous solutions when the applied pH value is several units above the relevant range, i.e. pH $\geq$ 4.

In a similar manner, one could propose the following hypotheses for the zeolite systems: firstly, acid/base equilibria of PFOA and/or sulfate radicals could be shifted to higher protonation degrees inside the zeolite pores than in the aqueous bulk phase. Van den Bergh et al. [11] suggested that PFOA adsorption in Al-free BEA zeolite may occur in the protonated form with specifically beneficial head-to-head interactions of PFOA molecules inside the zeolite. This hypothesis was mainly derived from DFT calculations (which however cannot take into account solvation/dissociation effects) and solid-state NMR results for dried PFOA-loaded zeolites.

Alternatively, acid catalysis by the zeolite surface could play a role, but cannot be assigned clearly to the content of acidic sites in zeolites due to the superposition of various effects.

Recently, Suehnholz et al. [33] described a heterogeneous activation of persulfate by FeS for oxidation of various organic compounds at ambient temperature. They suggest a surface-assisted homolytic bond cleavage of the O-O-bond in the peroxydisulfate dianion ($^{-}O_3S\text{-}O\cdots O\text{-}SO_3^{-}$) which proceeds with a low activation energy of $E_A = (31 \pm 1)$ kJ mol^{-1}. In a forthcoming study [34], these authors apply the system persulfate + FeS for the degradation of PFOA. Transferring this hypothesis to the system PFOA + persulfate + zeolite (instead of FeS), one could also postulate a surface-assisted persulfate activation in this case. This activation may promote the one-electron transfer from the PFOA carboxylate group to persulfate without attack of free sulfate radicals.

$$[C_7F_{15}COO^-]_{adsorbed} + [S_2O_8^{2-}]_{surface\ activated} \xrightarrow{e^- \text{ transfer}} C_7F_{15}COO\bullet + SO_4^{2-} + SO_4^{-}\bullet \qquad (16)$$

Such a hypothesis is in conformity with our observations: I) inhibition of n-octanol oxidation, which cannot be converted by electron transfer; II) absence of strong pH effects known for free sulfate radical-driven homogenous PFOA degradation by heat-activated persulfate; and III) insignificant acceleration of persulfate decomposition in the presence of zeolites. Based on the experimental results and mechanistic considerations, the proposed possible reaction pathways for PFOA degradation are further discussed in SI. Clearly, more research is needed in order to clarify the role of the zeolite in the accelerated PFOA degradation by heat-activated persulfate. The benefits of its combined role as adsorbent for PFOA removal and catalyst for subsequent degradation justify further detailed studies.

3.6. Stability and reusability test

As elucidated in chapter 3.2, PFOA degradation by heat-activated persulfate in the presence of zeolite is feasible under acidic to neutral conditions. Nevertheless, the decomposition of persulfate

inevitably decreases the pH value of the system, which could challenge the stability and reusability of the zeolites. Although decreasing the initial persulfate dosage could still ensure a complete PFOA degradation without a strong pH decrease, this would extend the reaction time. Controlling or buffering the system pH during the reaction would be another solution, with some additional efforts needed. However, Figure 8(c) shows that the zeolites maintained constant catalytic activities in PFOA degradation by heat-activated persulfate even after 6 runs without controlling the reaction pH during each cycle (detailed procedures are described in SI, Experimental Section). This shows that BEA35 indeed acts as a catalyst, and also indicates a good stability of the zeolite even under temporarily strongly acidic conditions (pH 1.5).

As shown in Figure 8 (a), a small amount of Al^{3+} (0.28 mg L^{-1} from 50 g L^{-1} zeolite) was leached out after 2 h adsorption. The Al^{3+} leaching increased with decreasing pH to 0.87 mg L^{-1} after 90-min reaction. After one reaction cycle, the leached Al^{3+} amount is approximately 0.12% of the total Al in the zeolite. The Al^{3+} leaching is strongest in the first run and then declines, becoming stable after the 3rd run with 0.09% of total Al per cycle. For practical application, a two-step process is most promising, whereby the zeolite is first used as adsorbent e.g. in a fixed-bed for treating contaminated water by safe and fast adsorption. Heat-activated persulfate would then be used only for regeneration of the fixed-bed, e.g., by in-circuit flushing with persulfate solution and heating of the bed. This low-volume regeneration solution can be post-treated by neutralization, whereby any leached Al^{3+} is precipitated as $Al(OH)_3$, and by adding Ca^{2+} to precipitate F^- as CaF_2.

3.7. Application to real water matrices and considerations for practical application

We have thus shown an efficient PFOA degradation by heat-activated persulfate in synthetic water in the presence of zeolites. In reality, ground and surface waters usually contain trace PFOA concentrations and complex water matrices, e.g. with coexisting organic compounds and inorganic

ions. For instance, chloride is reported to be a strong competitor for sulfate radicals [35]. As shown in Figure S11, we compared the PFOA degradation behavior by heat-activated persulfate in the presence of zeolites with and without addition of chloride. The addition of 5 mM chloride strongly inhibited the PFOA degradation, although its complete degradation can still be achieved after longer reaction times (> 6 h). Therefore, when dealing with real waters, a pretreatment (see Section 2.2) should be performed in order to: I) eliminate inorganic matrix components; and II) enrich the trace amount of PFOA from water. In this study, three groundwater samples were taken from three wells located in Leuna, a former refinery site in Germany. These groundwater samples contain trace amounts of PFOA, ranging from 35 to 82 ng L^{-1}. Detailed chemical composition of these groundwater samples, i.e. electrical conductivity, pH values, total organic carbon content and inorganic ions content, is presented in Table S1. Briefly, zeolite was added to groundwater samples for PFOA adsorption, precipitated by centrifugation and then the solid zeolite was transferred into DI water. In this way, most of the inorganic matrix components were excluded. The results in Figure 9(a) show that PFOA degradation by heat-activated persulfate is still applicable (PFOA degradation > 90% at t > 180 min) when dealing with trace PFOA in groundwater samples. Compared with PFOA in clean solution (Table 1), a decrease in $k_{obs,PFOA}$ was observed when PFOA had been previously extracted and concentrated on zeolite from groundwater. This was possibly due to competing degradation reactions of some organic compounds co-adsorbed in the zeolite (e.g. methyl *tert*-butyl ether and benzene), as the groundwater sample with the lowest DOC content showed the fastest PFOA degradation. In short, PFOA enrichment from a real groundwater sample can be achieved using zeolite, and combined with a subsequent heat-activated-persulfate PFOA degradation process.

Besides testing the degradation principle with real water, the economical consideration of this approach is also an important aspect that needs to be considered. Here we provide an initial estimate of the costs for treatment of PFOA-contaminated water in a realistic application scenario, i.e. using a zeolite fixed-bed adsorber, which is periodically regenerated by heat-activated persulfate (detailed cost estimate in SI). We estimated the total treatment costs, for zeolite, persulfate, and bed heating, to be in the range of 0.02–0.25 € m^{-3}. In addition, site-specific operational costs for groundwater pumping and reactor installation must be considered. The estimated operation cost is comparable to the prevailing large-scale PFAS *removal* technologies, i.e. ion exchange, activated carbon adsorption and reverse osmosis, with the groundwater pump-and-treat units operation costs of 0.8–1.7 € m^{-3}, 0.5–0.9 € m^{-3}, and 1.7-2.2 € m^{-3}, respectively [7].

In addition, it was also interesting to evaluate the reaction stoichiometric efficiency (% RSE) of the system. In the case where the system contained 100 mM persulfate, $C_{0,PFOA}$ = 240 mM, and $C_{zeolite}$ = 50 g L^{-1}, the RSE was calculated to be 3.6% when 90% PFOA degradation was achieved after 30 min. This value is higher than the RSE of 0.6% obtained in the homogenous heat-activated persulfate PFOA degradation at the same conditions. In this work, we designed the experiments with a high initial persulfate concentration in order to enable a fast degradation process while providing a proof-of-principle for a novel PFOA treatment approach. Accordingly, a relatively low RSE was obtained, which can certainly be improved at lower initial persulfate concentrations or step-wise dosing of persulfate as the oxidant itself acts as a consumer of sulfate radicals ($SO_4^{-}\cdot + S_2O_8^{2-} \longrightarrow SO_4^{2-} + S_2O_8^{-}\cdot$).

When we conducted the reaction at a 10-times lower initial persulfate dosage, the overall PFOA degradation rate declined (Figure 9(b)), but it still gave an adequate PFOA degradation efficiency (99.5%) at an extended reaction time of 4 h. The %RSE was calculated to be 12% when 90%

PFOA degradation was achieved after 2 h. Considering the rather low second-order rate constants ($k_{SO_4^{-}\cdot} = (1.7\text{-}4.4) \times 10^4$ $M^{-1}s^{-1}$) for reactions between PFCAs and sulfate radicals in aqueous solution [20], comparably low RSE values are expected. The relatively high RSE obtained in the presence of zeolite point to an additional reaction mechanism (in addition to the $SO_4^{-}\cdot$ attack) which may include $S_2O_8^{-}\cdot$. The role of this transient species needs to be explored in future studies. Nevertheless, in real applications, one can optimize the initial persulfate dosage and the corresponding reaction time such as to achieve a minimized chemicals and/or energy demand.

Although the BEA35 zeolite showed good performance not only in removing PFOA by adsorption, but also in accelerating its degradation by persulfate, thermal activation was still required to initiate this process. This is one limitation of the established approach. For *in situ* remediation of contaminated sites, it is desired to have an absorbent/catalyst able to adsorb traces of PFOA from e.g. contaminated aquifers, and activate injected persulfate at *in situ* relevant temperatures (about 12 °C). Thus, more investigations still needs to be done regarding the PFOA degradation under *in situ* relevant conditions in future studies.

4. Conclusion

This study presents an approach for a novel PFOA treatment technology, where PFOA can be firstly removed from water by zeolite adsorption, and then degraded directly in the adsorbed state by heat-activated persulfate. Overall, the major findings are summarized as follows:

I. Degradation by heat-activated persulfate is effective for PFOA adsorbed to a BEA-type zeolite, and a significant rate-enhancement was observed compared to the sulfate radical-based homogeneous system.

II. PFOA degradation by heat-activated persulfate in the presence of zeolite showed an adequate performance at initially neutral pH.

III. Zeolite internal surface promoted PFOA degradation by heat-activated persulfate. Further studies are needed in order to elucidate this catalytic effect, which may be due to reactive sites inside the zeolite.

IV. The stability and reusability of the zeolite were evaluated. After six adsorption/degradation cycles, BEA35 showed no significant decline in PFOA degradation performance.

V. Real groundwater samples containing PFOA in the ng L^{-1} range were found to be still effectively treated by the combination of zeolite adsorption and heat-activated persulfate.

VI. The costs for PFOA-contaminated water treatment were evaluated by applying a realistic scenario, i.e. a zeolite-based fixed-bed adsorber with intermittent regeneration by in-circuit flushing with persulfate solution at elevated temperature (70 °C). This preliminary estimation suggests that the approach can be cost-competitive to state-of-the-art processes, and deserves further research.

Acknowledgements

We thank Jieying Zhou for useful discussion and proof reading and Silke Woszidlo for technical support in conducting experiments. Lin Qian acknowledges financial support by China Scholarship Council.

Table 1. Adsorption and kinetic data on PFOA degradation with various BEA35 zeolite dosages (at pH_0 = 3.0, $C_{0,\ PFOA}$ = 240 μM, $C_{persulfate}$ = 100 mM, and T = 70 °C)

Zeolite dosages (g L^{-1})	**100**	**50**	**5**	**0.5**
$X_{Sorb,\ PFOA}$	0.999	0.998	0.985	0.58
q_{PFOA} **(g kg^{-1})** [a]	1.0	2.0	19	120
K_d **(L kg^{-1})** [b]	2.1×10^4	1.9×10^4	1.3×10^4	2.8×10^3
$k_{obs,PFOA}$ **(min^{-1})** [c]	0.098±0.007	0.077±0.004	0.063±0.012	0.030±0.001
PFOA $t_{1/2}$ (min)	6.6±0.5	8.5±0.4	9.2±1.8	22.0±1.0

[a] Sorbent loading.

[b] Single point adsorption coefficient K_d (L kg^{-1}) = q_{PFOA} (g kg^{-1}) / $C_{PFOA,free}$ (g L^{-1}).

[c] $k_{obs,PFOA}$ is obtained by first-order kinetics fitting within initial period of PFOA degradation (0 – 60 min). The error ranges are derived from the regression analysis of the data.

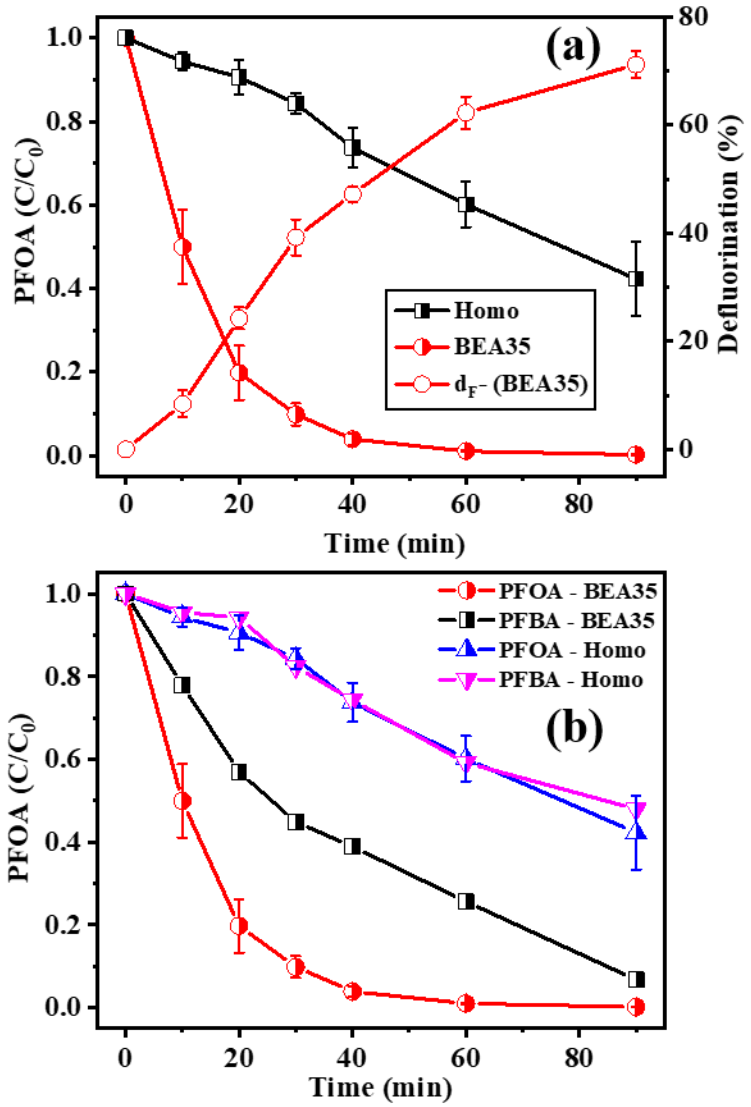

Figure 1. Comparison of heat-activated persulfate processes: (a) PFOA degradation with and without zeolite; (b) PFOA and PFBA degradation with and without zeolite. $C_{0,\mathrm{PFCAs}}$ = 240 μM, $C_{0,\mathrm{persulfate}}$ = 100 mM, pH_0 = 3.0, T = 70 °C, and C_{zeolite} = 50 g L^{-1} where applied. Error ranges represent mean deviations of single values from the mean of at least two experiments. Lines in plots of relative concentrations are added as guides for the eye.

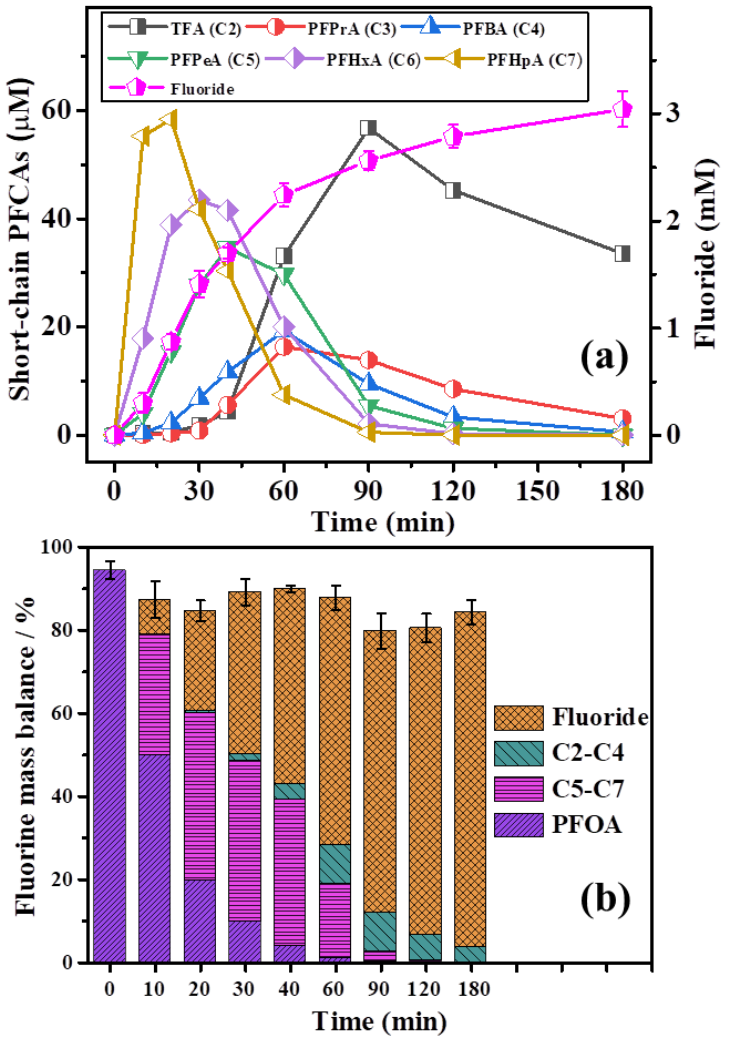

Figure 2. (a) Formation of short-chain PFCAs and fluoride during PFOA degradation by heat-activated persulfate; (b) Fluorine mass balance. The 0 min mass balance represents fluorine detected as PFOA in zeolite suspension determined by methanol extraction before start of reaction. The 180 min mass balance represents fluorine detected as C2 to C4 PFCAs and fluoride in the aqueous phase. $C_{zeolite}$ = 50 g L^{-1} and $C_{0,PFOA}$ = 240 μM, $C_{0,persulfate}$ = 100 mM, pH_0 = 3.0, and T = 70 °C. Error ranges represent mean deviations of single values from the mean of at least two experiments in Figure 2(a). The cumulative error is shown in Figure 2 (b). Lines in plots of relative concentrations are added as guides for the eye.

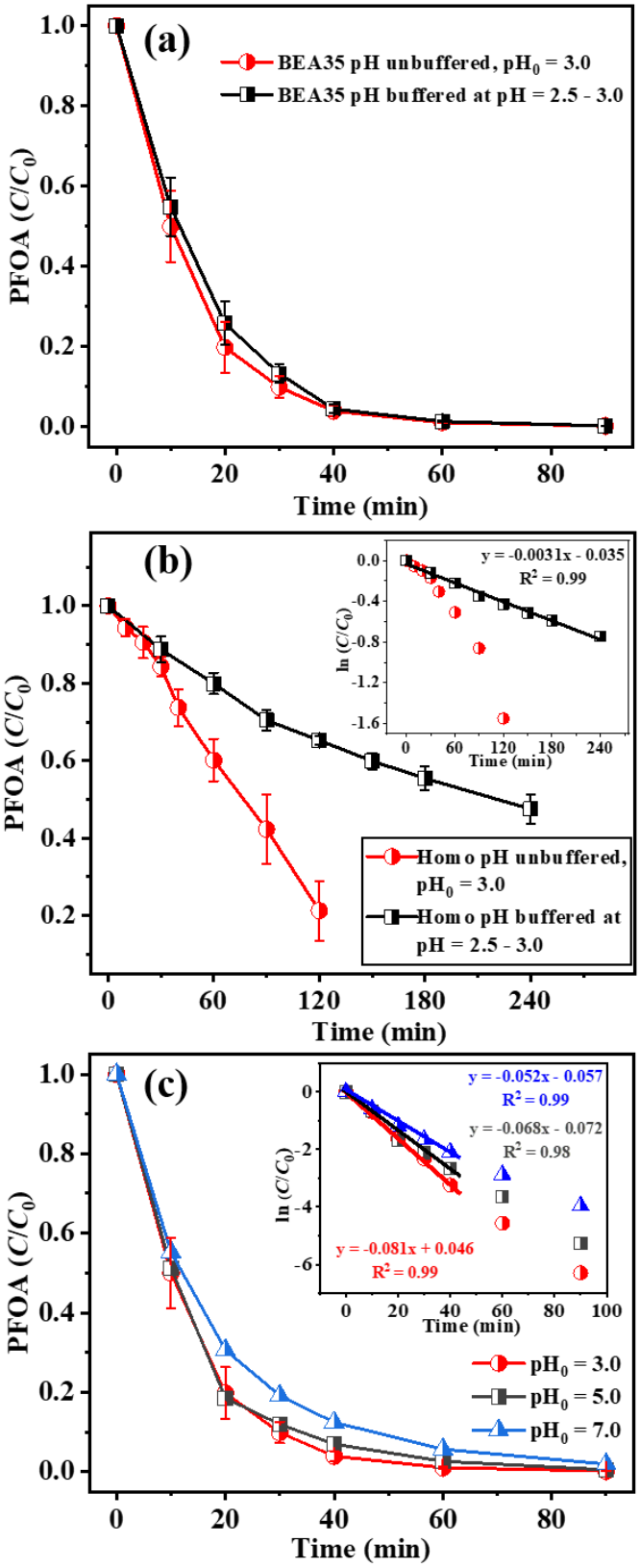

Figure 3. PFOA degradation by heat-activated persulfate: (a) effect of pH control in the presence

of zeolite; (b) effect of pH control in the absence of zeolite; (c) at various initial pH values in the presence of zeolite (no pH control). $C_{0,PFOA}$ = 240 μM, $C_{0,persulfate}$ = 100 mM, T = 70 °C, and $C_{zeolite}$ = 50 g L^{-1} where applied. Error ranges represent mean deviations of single values from the mean of at least two experiments. Lines in plots of relative concentrations are added as guides for the eye. Insets show fitting to pseudo-first order kinetics.

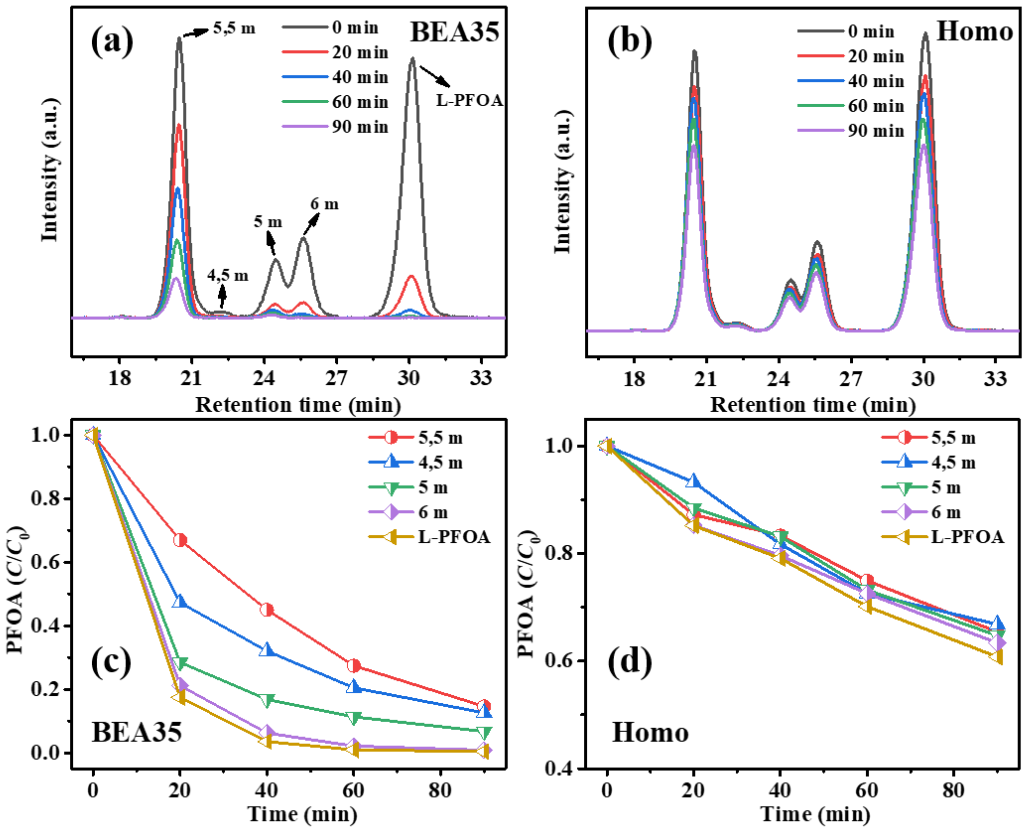

Figure 4. Some LC/MS chromatograms of samples from degradation of technical PFOA mixtures in the presence (a) and in the absence (b) of zeolite. Kinetics of degradation of technical PFOA mixtures in the presence (c) and absence (d) of zeolite. $C_{0,\text{persulfate}}$ = 100 mM, T = 70 °C, and C_{zeolite} = 50 g L^{-1} where applied. Lines in plots of relative concentrations are added as guides for the eye.

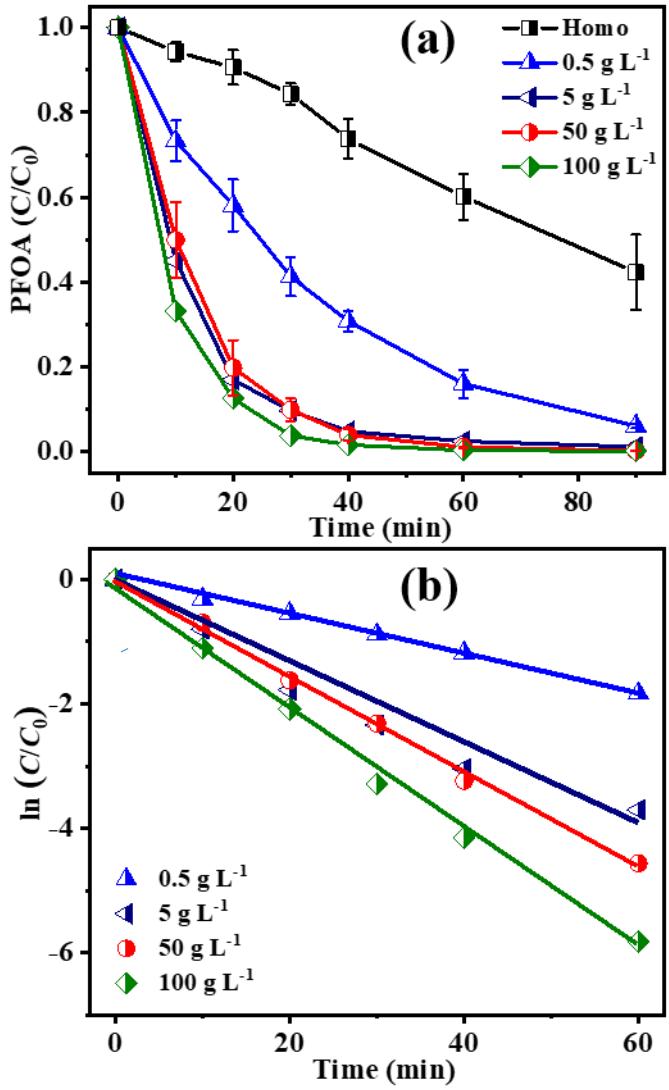

Figure 5. PFOA degradation by heat-activated persulfate with various zeolite dosages. $C_{0,PFOA}$ = 240 μM, $C_{0,persulfate}$ = 100 mM, pH_0 = 3.0, and T = 70 °C. (a) Residual concentrations over time and (b) pseudo-first order kinetics plots for initial reaction period (60 min). Error ranges represent mean deviations of single values from the mean of at least two experiments. Lines in (a) are added as guides for the eye.

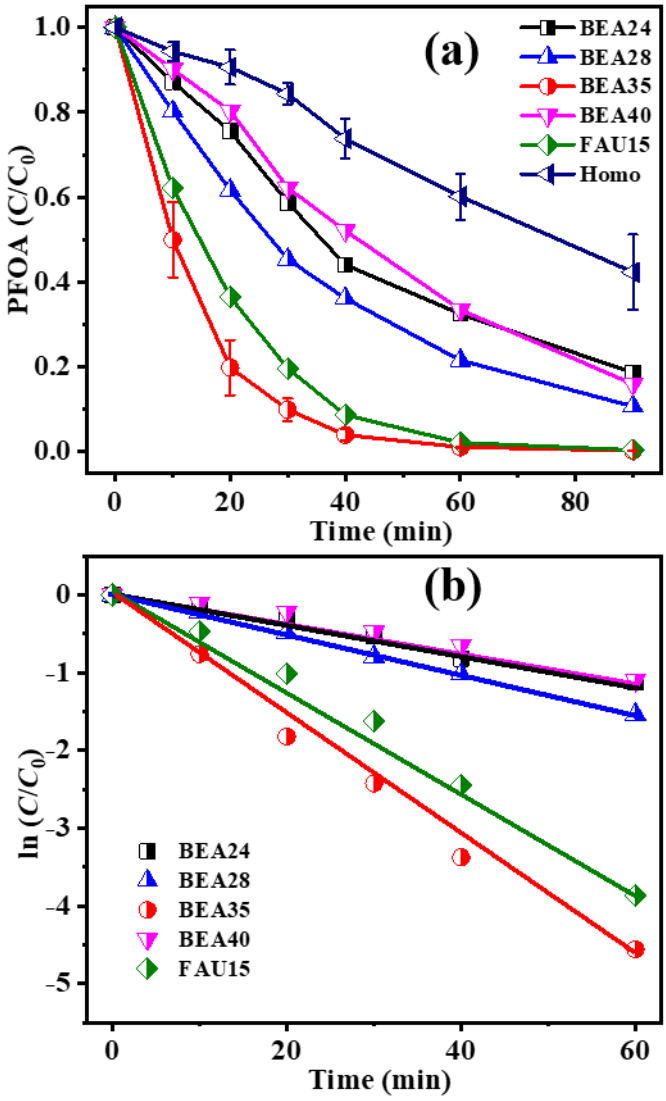

Figure 6. PFOA degradation by heat-activated persulfate with various types of zeolite. $C_{zeolite}$ = 50 g L^{-1}, $C_{0,PFOA}$ = 240 μM, $C_{0,persulfate}$ = 100 mM, pH_0 = 3.0, and T = 70 °C. (a) Residual concentrations over time and (b) pseudo-first order kinetics plots. Error ranges represent mean deviations of single values from the mean of at least two experiments. Lines in (a) are added as guides for the eye.

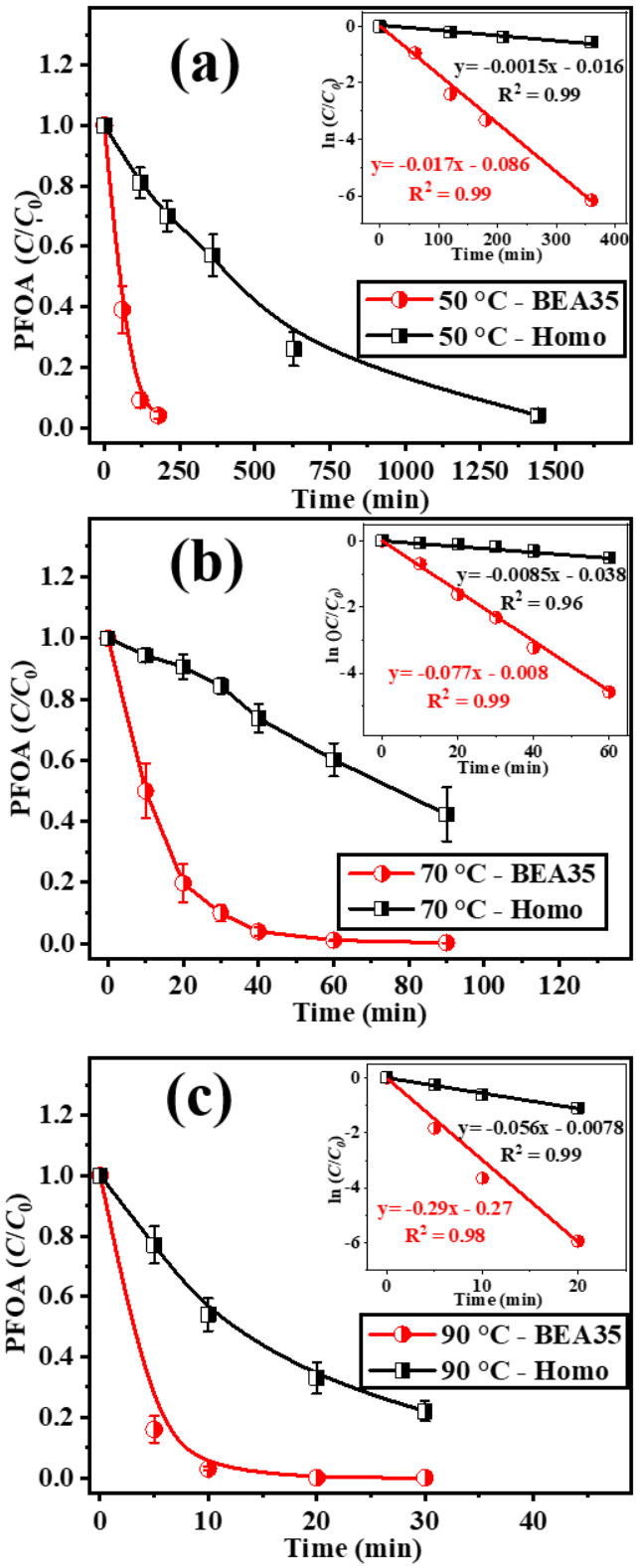

Figure 7. PFOA degradation by heat-activated persulfate at various activation temperatures.

$C_{0,PFOA}$ = 240 μM, $C_{0,persulfate}$ = 100 mM, pH_0 = 3.0, and $C_{zeolite}$ = 50 g L^{-1} where applied. Error ranges represent mean deviations of single values from the mean of at least two experiments. Lines in plots of relative concentrations are added as guides for the eye. Insets show fitting to pseudo-first order kinetics.

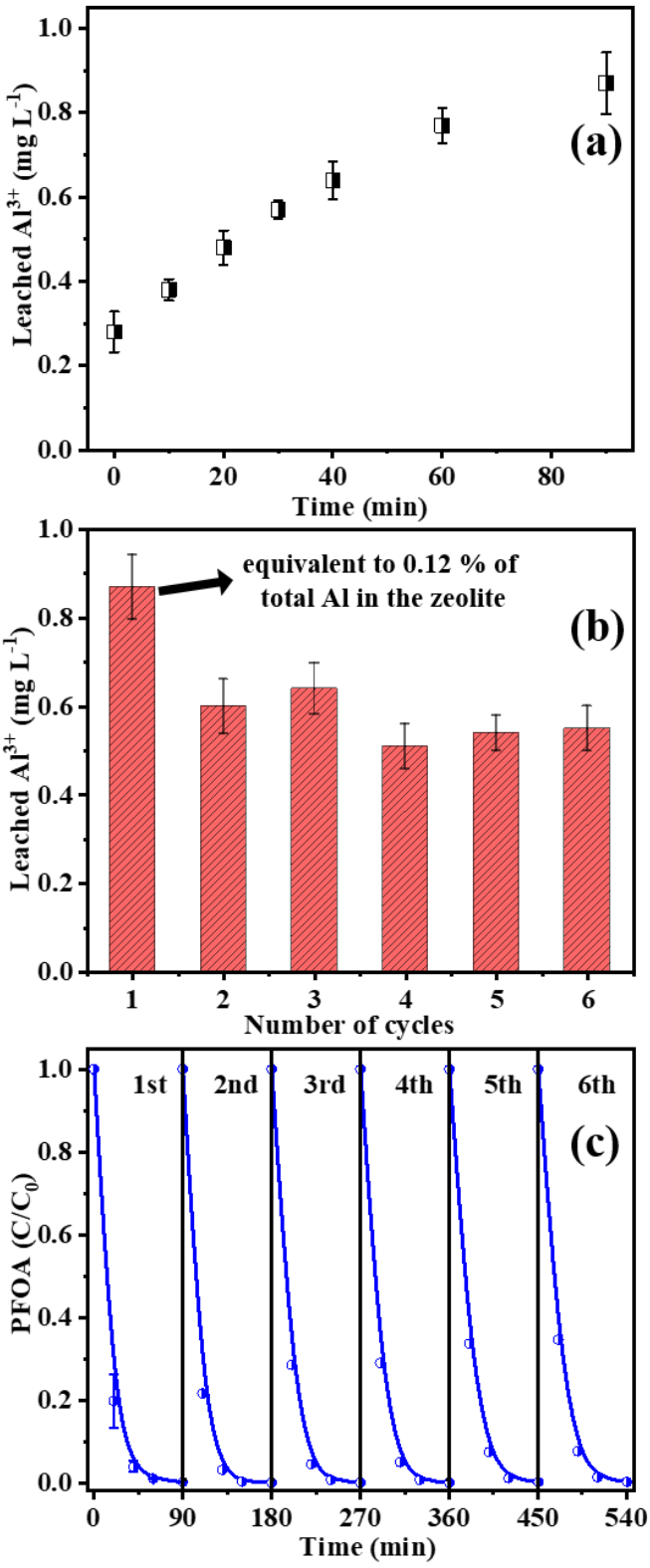

Figure 8. Aluminum leaching from zeolite BEA35 during PFOA degradation by heat-activated persulfate in the presence of zeolite: (a) in one cycle experiment; (b) in 6 consecutive batch runs.

(c) The reusability of BEA35 in 6 consecutive batch runs. $C_{zeolite}$ = 50 g L^{-1} and $C_{0,PFOA}$ = 240 μM each, $C_{0,persulfate}$ = 100 mM each, pH_0 = 3.0, and T = 70 °C. Error ranges represent mean deviations of single values from the mean of at least two experiments. Lines in plots of relative concentrations are added as guides for the eye.

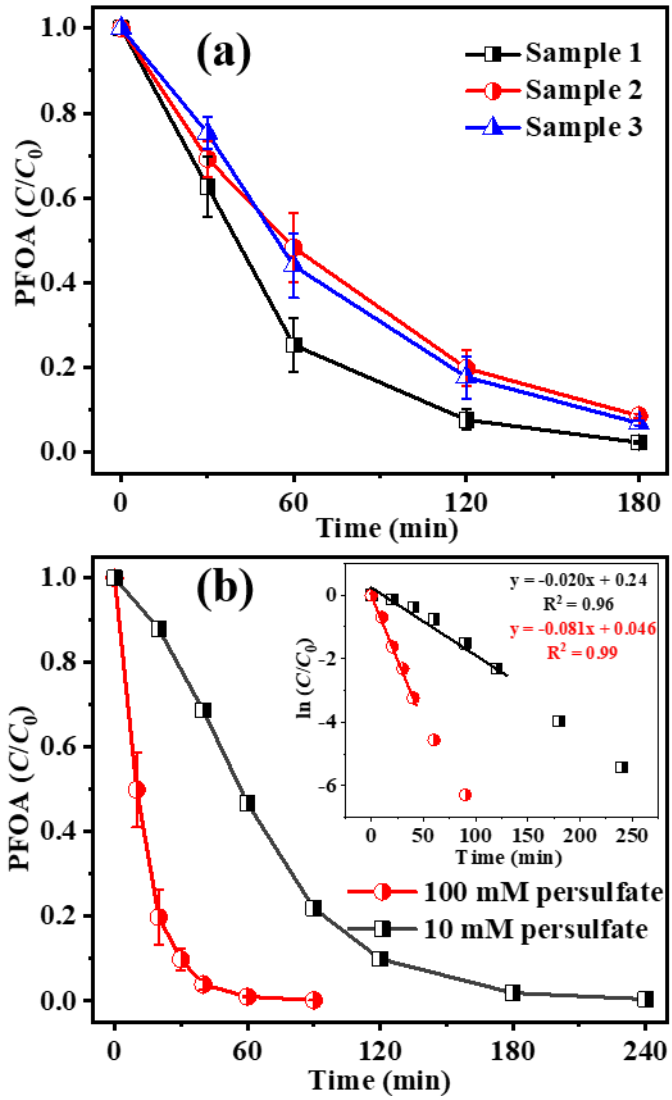

Figure 9. PFOA degradation by heat-activated persulfate in the presence of zeolite (a) with various groundwater samples, $C_{0,persulfate}$ = 100 mM; (b) with various initial persulfate dosages. $C_{zeolite}$ = 50 g L^{-1}, pH_0 = 3.0, and T = 70 °C. Error ranges represent mean deviations of single values from the mean of at least two experiments. Lines in plots of relative concentrations are added as guides for the eye. Inset shows fitting to pseudo-first order kinetics.

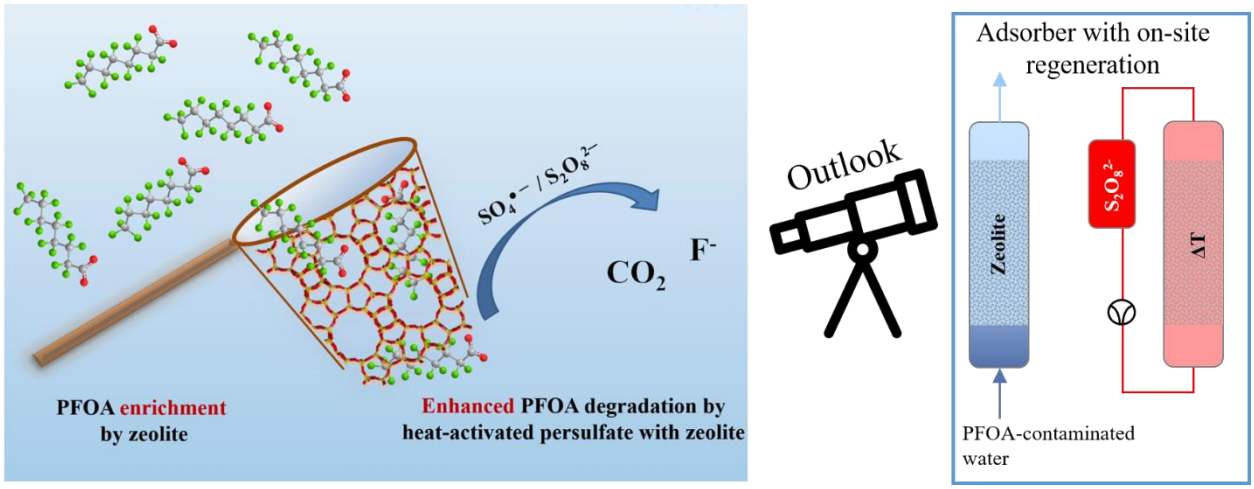

Graphical Abstract

References

[1] F. Xiao, T.R. Halbach, M.F. Simcik, J.S. Gulliver, Input characterization of perfluoroalkyl substances in wastewater treatment plants: Source discrimination by exploratory data analysis, Water Res. 46 (2012) 3101-3109. https://doi.org/10.1016/j.watres.2012.03.027

[2] V. Gallo, G. Leonardi, B. Genser, M.-J. Lopez-Espinosa, S.J. Frisbee, L. Karlsson, A.M. Ducatman, T. Fletcher, Serum perfluorooctanoate (PFOA) and perfluorooctane sulfonate (PFOS) concentrations and liver function biomarkers in a population with elevated PFOA exposure, Environ. Health Perspect. 120 (2012) 655-660. https://doi.org/doi:10.1289/ehp.1104436

[3] K. Steenland, S. Tinker, A. Shankar, A. Ducatman, Association of perfluorooctanoic acid (PFOA) and perfluorooctane sulfonate (PFOS) with uric acid among adults with elevated community exposure to PFOA, Environ. Health Perspect. 118 (2010) 229-233. https://doi.org/doi:10.1289/ehp.0900940

[4] A.G. Paul, K.C. Jones, A.J. Sweetman, A first global production, emission, and environmental inventory for perfluorooctane sulfonate, Environ. Sci. Technol. 43 (2009) 386-392. https://doi.org/10.1021/es802216n

[5] N. Yamashita, K. Kannan, S. Taniyasu, Y. Horii, G. Petrick, T. Gamo, A global survey of perfluorinated acids in oceans, Mar. Pollut. Bull. 51 (2005) 658-668. https://doi.org/10.1016/j.marpolbul.2005.04.026

[6] D. Huang, L. Yin, J. Niu, Photoinduced hydrodefluorination mechanisms of perfluorooctanoic acid by the SiC/Graphene catalyst, Environ. Sci. Technol. 50 (2016) 5857-5863. https://doi.org/10.1021/acs.est.6b00652

[7] H.-G. Edel, D.-I.D. Klopp, B.E.J. Drubel, B.E.D. Korte, D.-I.C. Kellner, D.-I.U. Rehnig, PFAS Groundwater remediation: State of the art technology and comparison of costs - English translation of reprint from Handbuch Altlastensanierung und Flachenmanagement (HdA).

[8] M. Trojanowicz, A. Bojanowska-Czajka, I. Bartosiewicz, K. Kulisa, Advanced oxidation/reduction processes treatment for aqueous perfluorooctanoate (PFOA) and perfluorooctanesulfonate (PFOS) – a review of recent advances, Chem. Eng. J. 336 (2018) 170-199. https://doi.org/10.1016/j.cej.2017.10.153

[9] H. Hori, A. Yamamoto, E. Hayakawa, S. Taniyasu, N. Yamashita, S. Kutsuna, H. Kiatagawa, R. Arakawa, Efficient decomposition of environmentally persistent perfluorocarboxylic acids by use of persulfate as a photochemical oxidant, Environ. Sci. Technol. 39 (2005) 2383-2388. https://doi.org/10.1021/es0484754

[10] H. Hori, Y. Nagaoka, M. Murayama, S. Kutsuna, Efficient decomposition of perfluorocarboxylic acids and alternative fluorochemical surfactants in hot water, Environ. Sci. Technol. 42 (2008) 7438-7443. https://doi.org/10.1021/es800832p

[11] S. Naim, A. Ghauch, Ranitidine abatement in chemically activated persulfate systems: Assessment of industrial iron waste for sustainable applications, Chem. Eng. J. 288 (2016) 276-288. https://doi.org/10.1016/j.cej.2015.11.101

[12] A. Ghauch, G. Ayoub, S. Naim, Degradation of sulfamethoxazole by persulfate assisted micrometric Fe0 in aqueous solution, Chem. Eng. J. 228 (2013) 1168-1181. https://doi.org/10.1016/j.cej.2013.05.045

[13] G. Ayoub, A. Ghauch, Assessment of bimetallic and trimetallic iron-based systems for persulfate activation: Application to sulfamethoxazole degradation, Chem. Eng. J. 256 (2014) 280-292. https://doi.org/10.1016/j.cej.2014.07.002

[14] S.X. Liang, Z. Jia, W.C. Zhang, X.F. Li, W.M. Wang, H.C. Lin, L.C. Zhang, Ultrafast activation efficiency of three peroxides by $Fe_{78}Si_9B_{13}$ metallic glass under photo-enhanced catalytic oxidation: A comparative study, Appl. Cat. B: Environ. 221 (2018) 108-118. https://doi.org/10.1016/j.apcatb.2017.09.007

[15] S.-X. Liang, X. Wang, W. Zhang, Y.-J. Liu, W. Wang, L.-C. Zhang, Selective laser melting manufactured porous Fe-based metallic glass matrix composite with remarkable catalytic activity and reusability, Appl. Mater. Today 19 (2020) 100543. https://doi.org/10.1016/j.apmt.2019.100543

[16] J. Wu, B. Wang, G. Cagnetta, J. Huang, Y. Wang, S. Deng, G. Yu, Nanoscale zero valent iron-activated persulfate coupled with Fenton oxidation process for typical pharmaceuticals and personal care products degradation, Sep. Purif. Technol. 239 (2020) 116534. https://doi.org/10.1016/j.seppur.2020.116534

[17] A. Baalbaki, N. Zein Eddine, S. Jaber, M. Amasha, A. Ghauch, Rapid quantification of persulfate in aqueous systems using a modified HPLC unit, Talanta 178 (2018) 237-245. https://doi.org/10.1016/j.talanta.2017.09.036

[18] O. Tantawi, A. Baalbaki, R. El Asmar, A. Ghauch, A rapid and economical method for the quantification of hydrogen peroxide (H_2O_2) using a modified HPLC apparatus, Sci. Total Environ. 654 (2019) 107-117. https://doi.org/10.1016/j.scitotenv.2018.10.372

[19] R. El Asmar, A. Baalbaki, Z. Abou Khalil, S. Naim, A. Bejjani, A. Ghauch, Iron-based metal organic framework MIL-88-A for the degradation of naproxen in water through persulfate activation, Chem. Eng. J. 405 (2021) 126701. https://doi.org/10.1016/j.cej.2020.126701

[20] H.V. Lutze, J. Brekenfeld, S. Naumov, C. von Sonntag, T.C. Schmidt, Degradation of perfluorinated compounds by sulfate radicals – New mechanistic aspects and economical considerations, Water Res. 129 (2018) 509-519. https://doi.org/10.1016/j.watres.2017.10.067

[21] M. Van den Bergh, A. Krajnc, S. Voorspoels, S.R. Tavares, S. Mullens, I. Beurroies, G. Maurin, G. Mali, D.E. De Vos, Highly selective removal of perfluorinated contaminants by adsorption on all-silica zeolite beta, Angew. Chem. Int. Ed. 59 (2020) 14086-14090. https://doi.org/10.1002/anie.202002953

[22] L. Qian, F.-D. Kopinke, A. Georgi, Photodegradation of perfluorooctanesulfonic acid on Fe-zeolites in water, Environ. Sci. Technol. 55 (2021) 614-622. https://doi.org/10.1021/acs.est.0c04558

[23] L. Qian, A. Georgi, R. Gonzalez-Olmos, F.-D. Kopinke, Degradation of perfluorooctanoic acid adsorbed on Fe-zeolites with molecular oxygen as oxidant under UV-A irradiation, Appl. Cat. B: Environ. 278 (2020) 119283. https://doi.org/10.1016/j.apcatb.2020.119283

[24] B. Sun, J. Ma, D.L. Sedlak, Chemisorption of perfluorooctanoic acid on powdered activated carbon initiated by persulfate in aqueous solution, Environ. Sci. Technol. 50 (2016) 7618-7624. https://doi.org/10.1021/acs.est.6b00411

[25] C. Liang, C.-F. Huang, N. Mohanty, R.M. Kurakalva, A rapid spectrophotometric determination of persulfate anion in ISCO, Chemosphere 73 (2008) 1540-1543. https://doi.org/10.1016/j.chemosphere.2008.08.043

[26] S. Kutsuna, H. Hori, Rate constants for aqueous-phase reactions of SO_4^- with $C_2F_5C(O)O^-$ and $C_3F_7C(O)O^-$ at 298 K, Int. J. Chem. Kinet. 39 (2007) 276-288. https://doi.org/10.1002/kin.20239

[27] T.A. Bruton, D.L. Sedlak, Treatment of perfluoroalkyl acids by heat-activated persulfate under conditions representative of in situ chemical oxidation, Chemosphere 206 (2018) 457-464. https://doi.org/10.1016/j.chemosphere.2018.04.128

[28] R.C. Buck, J. Franklin, U. Berger, J.M. Conder, I.T. Cousins, P. de Voogt, A.A. Jensen, K. Kannan, S.A. Mabury, S.P. van Leeuwen, Perfluoroalkyl and polyfluoroalkyl substances in the environment: Terminology, classification, and origins, Integr. Environ. Assess. Manag. 7 (2011) 513-541. https://doi.org/10.1002/ieam.258

[29] W. Kim, J.-C. Kim, J. Kim, Y. Seo, R. Ryoo, External surface catalytic sites of surfactant-tailored nanomorphic zeolites for benzene isopropylation to cumene, ACS Catal. 3 (2013) 192-195. https://doi.org/10.1021/cs300678n

[30] C.L. Clifton, R.E. Huie, Rate constants for hydrogen abstraction reactions of the sulfate radical, SO_4^-. alcohols, Int. J. Chem. Kinet. 21 (1989) 677-687. https://doi.org/10.1002/kin.550210807

[31] K.-U. Goss, The pK_a values of PFOA and other highly fluorinated carboxylic acids, Environ. Sci. Technol. 42 (2008) 456-458. https://doi.org/10.1021/es702192c

[32] A. Baggioli, M. Sansotera, W. Navarrini, Thermodynamics of aqueous perfluorooctanoic acid (PFOA) and 4,8-dioxa-3H-perfluorononanoic acid (DONA) from DFT calculations: Insights into degradation initiation, Chemosphere 193 (2018) 1063-1070. https://doi.org/10.1016/j.chemosphere.2017.11.115

[33] S. Sühnholz, F.-D. Kopinke, K. Mackenzie, Reagent or catalyst? – FeS as activator for persulfate in water, Chem. Eng. J. 387 (2020) 123804. https://doi.org/10.1016/j.cej.2019.123804

[34] S. Sühnholz, A. Gawel, F.-D. Kopinke, K. Mackenzie, Evidence of heterogeneous degradation of PFOA by activated persulfate – FeS as adsorber and activator, Chem. Eng. J. (2021) 130102. https://doi.org/10.1016/j.cej.2021.130102

[35] H.V. Lutze, N. Kerlin, T.C. Schmidt, Sulfate radical-based water treatment in presence of chloride: Formation of chlorate, inter-conversion of sulfate radicals into hydroxyl radicals and influence of bicarbonate, Water Res. 72 (2015) 349-360. https://doi.org/10.1016/j.watres.2014.10.006